established in 2016

MAS JOURNAL of Applied Sciences

ISSN 2757-5675

DOI: http://dx.doi.org/10.52520/masjaps.120

Araştırma Makalesi

Biosynthesis of Black Mulberry Leaf Extract and Silver NanoParticles (AgNPs): Characterization, Antimicrobial and Cytotoxic Activity Applications

Necmettin AKTEPE*[1], Ayşe BARAN[2], Mehmet Nuri ATALAR[3], Mehmet Fırat BARAN[4], Cumali KESKİN[4], Mehmet Zahir DÜZ[5], Ömer YAVUZ[5], Sevgi İRTEGUN KANDEMİR[6], Deniz Evrim KAVAK[7]

[1]Mardin Artuklu University, Department of Nursing, Artuklu/Mardin
[2]Mardin Artuklu University graduate education institute Department of Biology, Mardin
[3]Department of Nutrition and Dietetics, Faculty of Health Science, Igdir University, Igdir
[4]Medical Laboratory Techniques Vocational Higher School of Healthcare Studies, Mardin
[5]Dicle University, Faculty of Science, Department of Chemistry, Diyarbakir
[6]Department of Medical Biology, Faculty of Medicine, Dicle University, Diyarbakir
[7]Dicle University Science and Technology Research Center, Dicle University, Diyarbakir

*Sorumlu yazar: necmettinaktepe@gmail.com

Geliş Tarihi: 19.03.2021 **Kabul Tarihi**: 24.04.2021

Abstract

The fact that AgNPs are obtained by biosynthesis applications are simple, economical and environmentally friendly are the reasons why the interest in these synthesis methods is increasing day by day. In this study, AgNPs were rapidly synthesized using the extract created from *Morus nigra L.* leaves. The application stages were carried out in room conditions without requiring special conditions. AgNPs were characterized using various instrument data. Maximum absorbance of AgNPs at 417.47 nm wavelength in UV-visible spectrophotometer (UV-Vis.), Crystal nanosize and crystal structures of 23.29 nm in X-Ray Diffraction Diffractometer (XRD), Scanning Electron Microscope (SEM) and Transmission Electron Microscopy (TEM) micrographs, it was determined that they had a spherical appearance, they had a stable structure with negative charge distribution with -25.01 mV Zeta potential data, and that there was no aggregation. Fourier Transform Infrared Spectroscopy (FTIR) data demonstrated the phytochemicals involved in reduction and X-ray Energy Dispersive Difratrometer (EDX) with strong silver peaks indicating the presence of AgNPs. Suppressive activities of AgNPs on growth of pathogen strains were determined by microdilution method with Minimum Inhibition Concentration (MIC). Cytotoxic activities were investigated by MTT method on healthy cell lines and different cancer cell lines.

Keywords: AgNPs, Biosynthesis, MTT method, MIC, TEM

1. INTRODUCTION

Metallic nanoparticles are valuable materials. Silver (Ag) (Eren, A., Baran, 2019a), gold (Au) (Baran, M. F., Saydut, 2019), zinc (Zn) (Doğaroğlu et al., 2019), copper (Cu) (El-Batal et al., 2018), palladium (Pd) (El-Batal et al., 2018) are some of them. They have superior physical and chemical properties such as having a large surface area and being resistant to high heat treatments. Different recovery methods such as chemical, physical and biosynthesis are used to obtain metallic nanoparticles. Biosynthesis methods are environmentally friendly, cheap and easy, which increases the interest in this synthesis. The fact that biosynthesis methods are environmentally friendly, cheap and easy increases the interest in this synthesis (Ojo, O.A., Oyinloye, B.E., Ojo, A.B., Afolabi, O.B., Peters, O.A., Olaiya, O., Fadaka, A., Jonathan, j., Osunlana, 2017), (M. F. Baran, 2018). AgNPs have many uses such as bioremediation studies (Thomas et al., 2018), catalysis studies (Singh et al., 2018), biomedical applications (Ramkumar et al., 2017), food industry (Velmurugan et al., 2014), cosmetics industry (Arroyo et al., 2020). Sources used in biosynthesis include plants (Ferreyra Maillard et al., 2018), bacteria (Gopalu, K., Matheswaran J., Alexander, G., Juan, Antonio LT., Evgeny, K., 2016), fungi (S, Majeed., Mohd, S. A., Gouri K. D., Mohammed, T.A., Anima, 2016), algae (Mousavi et al., 2019). Biosynthesis with plants is faster, more stable, yields high and does not carry risks such as pathogenicity. Also, no special conditions are required to obtain it. Parts of the plant itself (M. Ali et al., 2016) or parts such as leaves (Francis et al., 2017), roots (Mohammadi et al., 2019), fruit pods (M. H. Ali, 2020), flowers (Patil et al., 2018) can be used for biosynthesis. Phytochemicals such as alcoholloids (Kumar, R., Ghoshal, G. Jain, 2017), flavonoids (Kumar, R., Ghoshal, G. Jain, 2017), terpenoids (Remya et al., 2015), phenolic compounds (Gupta et al., 2018) found in the structure of plant sources, form AgNPs by reducing Ag^{+} ions in the aqueous environment by providing Ag^{o} formation. Various studies are carried out on how AgNPs can be used as an alternative treatment source by taking them as anti-microbial and anti-cancer agents in the pharmacology industry (Al-ogaidi et al., 2017), (Arumai Selvan et al., 2018). Various studies are carried out on AgNPs in the pharmacology industry by taking them as anti-microbial and anti-cancer agents and becoming an alternative treatment source. These researches can contribute to both the fight of many people against microorganisms that develop resistance to the antibiotics and the treatments of many cancer patients. Black mulberry (*Morus nigra L.*) is a plant from the Moraceae family, whose secondary metabolic products are used for many purposes. Black mulberry leaves are a plant used in conditions such as diabetes, inflammation, cough, fever. It is rich in bioactive components such as polyphenols and phlovanoids (Hafez et al., 2017), (A. Kumar et al., 2013). In this study, it was aimed to investigate the economical, easy and fast biosynthesis, characterization, antimicrobial and cytotoxic activities of AgNPs with the extract prepared using the leaves of *Morus nigra L.*

2. MATERIALS and METHODS

2.1. Preparation of Morus nigra L. leaf extract and 5 mM AgNO3 (silver nitrate) solution

The leaves of *Morus nigra L.* were collected in the Mardin Mazıdağ region at the end of August. The collected leaves were washed several

times with tap water. Afterwards, a few more washing processes were carried out using distilled water. It was dried in room conditions. 100 g of dried leaves were weighed and mixed with 750 ml of distilled water and left to boil. The extract to be used for synthesis was prepared by cooling and filtering using filter paper. 5 mM (millimolar) solution was prepared freshly with Sigma aldrich brand solid AgNO3 salt to be used in the preparation of AgNPs before starting the synthesis.

2.2. Biosynthesis of AgNPs

250 mL of *Morus nigra L.* leaf extract and 750 mL of 5 mM AgNO3 solution were mixed and kept at room temperature (22 ^{o}C) for biosynthesis.

2.3. Characterization of AgNPs

Perkin Elmer One brand UV-Vis due to color change occurring 20 minutes after mixing leaf extract and 10 mM (millimolar) $AgNO_3$ solution. Maximum absorbance data were examined by performing wavelength scans in the range of 200-800 nm in order to detect the formation of AgNPs with the spectrophotometer device (Shao et al., 2018). In order to evaluate the frequencies of the groups of phytochemicals responsible for effective reduction in the formation of AgNPs, the data of the leaf extract and the reaction liquid formed after the synthesis were evaluated using a Perkin Elmer One brand FT-IR device. The crystal structures and nano sizes of AgNPs were determined with the data obtained from the measurements made on Rigaku Miniflex 600 model computer controlled XRD device 2θ. The nano size was calculated using the Debye-Scherrer formula given below (Eren, A., Baran, 2019a).

$$\mathbf{D = K\lambda / (\beta \cos\theta)} \quad (1)$$

In the formula, D = particle size, K = constant value, λ = X-ray wavelength value, β = half of the FWHM value of the peak with maximum height, θ = Bragg angle of the high peak. The morphological structures of AgNPs were determined with EVO 40 LEQ SEM and Jeol Jem 1010 TEM micrographs. The elemental composition of the particles was determined with the RadB-DMAX II computer controlled EDX device data. In addition, Zeta potential and charge distributions were determined using the Malvern device to determine the surface load structures of AgNPs.

2.3. Examination of the antimicrobial activities of AgNPs by Microdilution method

In order to determine the anti-microbial effects of AgNPs, MIC determination was performed on pathogen gram positive and negative bacteria as well as on yeast by using micro dilution method. *Staphylococcus aureus* (*S. aureus*) *ATCC 29213*, *Escherichia coli* (*E. coli*) *ATCC25922* and *Candida albicans* (*C. albicans*) strains were procured from the Microbiology Laboratory of İnönü University Medical Faculty Hospital. *Bacillus subtilis* (*B. subtilis*) *ATCC 11774* and *Pseudomonas aeruginosa* (*P. aeruginosa*) *ATCC27833* strains were also procured from Mardin Artuklu University Microbiology Research Laboratory. Gram positive bacteria *S. aureus* and *B. Subtilis* and gram negative bacteria *E. coli* and *P. aeruginosa* bacteria were grown on nutrient agar solid media plates at 37 oC overnight. Yeast C. albicans was also grown on Sabora dextros agar medium. Subsequently, microorganism suspensions were prepared for each according to McFarland standard 0.5 (Emmanuel et al., 2015) turbidity concentration using microorganisms grown on the medium plates. For micro dilution, media suitable for each microorganism was pipetted into 96 microplates. Muller hinton broth was

added for application with bacteria and Roswell Park Memorial Institute (RPMI) medium for Maya C. albicans. One well was determined for sterilization and one well for growth control. The solution prepared with AgNPs at a concentration of 16 µg/mL^{-1} was put into the first well. Micro dilution was applied to the other wells starting from the first well. Then, the suspensions prepared according to Mc Farland 0.5 turbid standard for each microorganism were added to the micro-diluted microplate wells. After these procedures, the microplates were incubated at 37 ºC overnight. The next day, the wells in the microplates were examined one by one and the concentration of the well before the well where the growth started was determined as MIC.

2.4. Cytotoxic Activities of AgNPs in cell lines by MTT method

The cytotoxic effects of AgNPs synthesized with *Morus nigra L.* leaf extract in the Cell Culture Laboratory of Dicle University Scientific Research Center by MTT method using supply cell lines from the American Type Culture Collection (ATCC) were performed. In practice, different cell lines were studied, one of which was a healthy cell line. Human Dermal Fibroblast (HDF) was used as a healthy cell line. Human Colorectal Adenocarcinoma (Caco-2), Glioblastoma (U118) and Human Ovarian sarcoma (Skov-3) were used as cancer cell lines. All cell lines were cultured in 75 t-flasks. Culture media DMEM (Dulbecco Modified Eagle) medium with HDF, 10% FBS 2 mM L-Glutamine and 100 U / ml Penstrep for HDF, CaCo-2 and U118 cell lines, 10% FBS for Ovarian sarcoma (Skov-3) cell lines, RPMI (Roswell Park Memorial Institute) 1640 medium containing 100 U/ml Penstrep was used. Flasks cultured with cell lines were incubated in a 37 ° C oven containing 5% CO2, 95% air, humidity. After cells reached about 80% confluence, cells were counted with a hemocytometer, inoculating 10^4 cells per well of 96-well plates and incubating overnight. After the incubation period, cells were treated with nanoparticles at varying concentrations of 25-200 µg / mL^1 and incubated for 48 hours. Untreated cells were used as control. After incubation, MTT solution was added to each well and incubated for 3 hours. After the incubation, the medium in the wells was slowly aspirated with MTT reagent. Then 100 µl of DMSO was added to each well and left for a further 15 minutes at room temperature with gentle shaking. The absorbance of the microplates at 540 nm wavelength was measured using the Multi ScanGo, Thermo device.

$\%\ \text{viability} = U/C * 100$ (Remya et al., 2015) (1)

In the formula, U; Absorbance values of cells treated with AgNPs, C; expresses the absorbance values of control cells.

3. FINDINGS and DISCUSSION

3.1. UV-visible spectroscopy

Leaf extract of *Morus nigra L.* and 5 mM $AgNO_3$ solution were mixed, and after 15 minutes the color change began to occur, as time passed, a transformation from yellow to dark brown was observed (Z. A. Ali et al., 2016), (Song & Kim, 2009). The color change from yellow to brown occurs as a result of vibrations (SPR) occurring on the plasma surface due to the formation of AgNPs (Ahmed et al., 2019), (M. F. Baran, 2018). UV-vis by sampling depending on the intensity of color change. device, the maximum absorbance value was found at 417.47 nm as a result of wavelength scans (Figure 1). It has been stated that AgNPs obtained with Mussaenda glabrata extract give maximum absorbance at 415 nm (Francis et al., 2017). In other biosynthesis studies,

absorbances at wavelengths of 415 nm (Butola et al., 2019) and 418 nm (Shao et al., 2018) have been characterized by the presence of AgNPs.

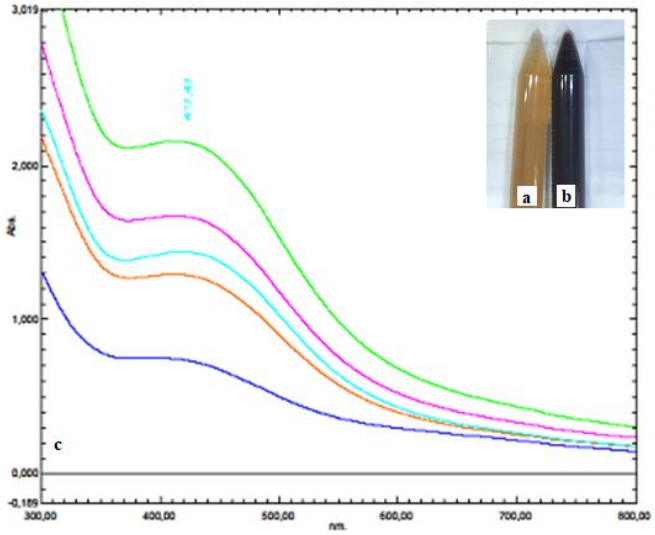

Figure 1. a. Leaf extract **b.** Dark brown color change due to the Formation of AgNPs, **c.** UV-vis indicating the presence of AgNPs spectrophotometer data

3.2. XRD Analysis Data

The crystal structure and nano dimensions of AgNPs were determined with the peaks and values of 111°, 200°, 220° and 311° as a result of the analysis performed with XRD device at 2θ. These peaks indicate that AgNPs are in cubic crystal structure (Rouhollah, H., and Marzieh, 2014), (Khan et al., 2018). The FWHM values of 111°, 200°, 220° and 311° peaks are 38.07, 44.30, 64.44 and 77.40, respectively, of the crystal structure of silver. The data show that the AgNPs obtained have a cubic crystal structure (Figure 2). By using the values of the spectra read in 2θ, the crystal nano sizes of AgNPs were calculated with the Debye-Scherrer equation (Khan et al., 2018).

$$D=K\lambda/(\beta\cos\theta) \quad (2)$$

In Equation (2), D = particle size, K constant value (0.90), λ = X-ray wavelength value (1.5418 Å), β = FWHM value of the high peak, cosθ = Braggθ angle of the high peak.

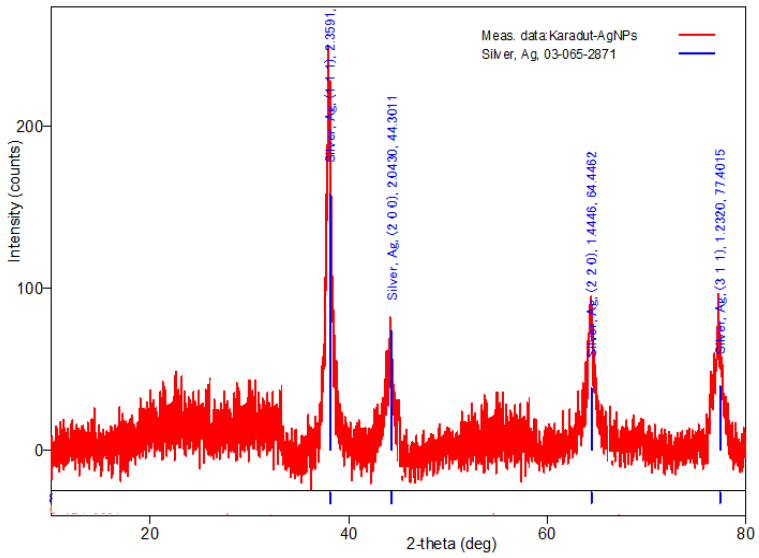

Figure 2. XRD pattern of the crystal structures of AgNPs

As a result of the calculation, it was concluded that the crystal nano size was 23.29 nm. In other studies calculating the crystal nano size of AgNPs using the Debye-Scherrer equation, dimensions of 18 nm (Vastrad, 2016) and 20 nm (Pugazhendhi et al., 2018) were found.

3.3. FT-IR spectroscopy data

FTIR spectroscopy data of both the plant extract and the post-synthesis reaction fluid to identify the functional groups of phytochemicals involved in reduction are shown in Figure 3. 3334.52-3333. 55 cm-1, 2107.4--2108. There were shifts in spectral frequencies of 24 cm-1 and 1635.5–1635.21 cm-1. Functional groups belonging to these frequencies may have led to the formation of AgNPs by reducing the Ag^{+} ion to the Ag^{o} form. The frequency shifts at three points suggest that -OH (hydroxyl) (Eren, A., Baran, 2019b), C≡C (alkyne) (Baran, M.F., Koç, A., and Uzan, 2018) and -NH2 (amine) functional groups, respectively, are effective in reduction. However, these functional groups also ensure the stability of the synthesis (V. Kumar et al., 2016) (Figure 3).

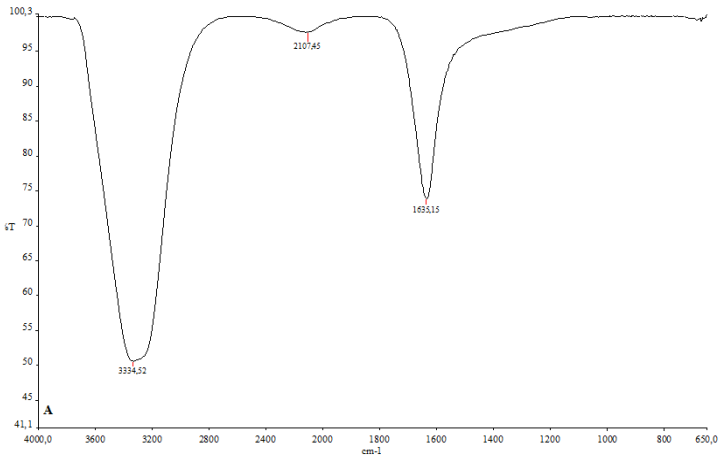

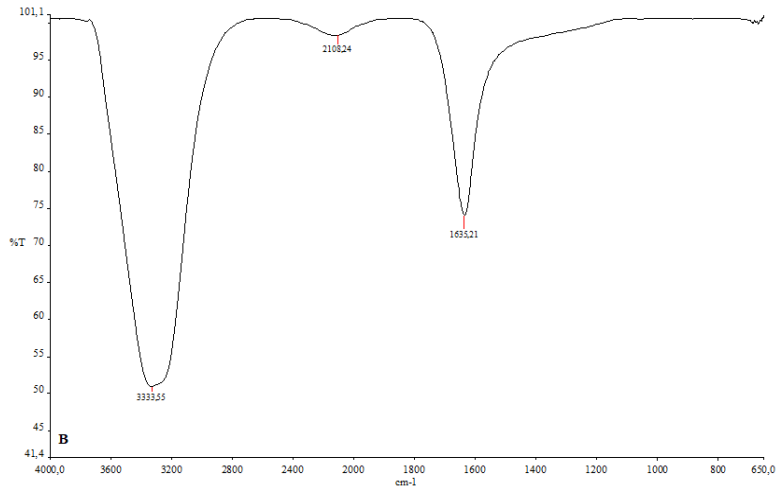

Figure 3. A. FTIR spectra of *Morus nigra L.* leaf extract, **B.** spectrum data of the liquid medium obtained after the synthesis of AgNPs

3.4. SEM, TEM micrographs and EDX profile of AgNPs

In Figure 4A, B, it was shown that the morphology of AgNPs obtained as a result of biosynthesis with *Morus nigra L.* extract had a spherical view in SEM and TEM micrographs (Butola et al., 2019), (M. Baran, 2019). Strong peaks of silver in the EDX graph for element composition show the presence of AgNPs (V. Kumar et al., 2016). In addition, weak C, Cl and O peaks in EDX graph suggest that AgNPs, which are bound to the phytochemicals coming from the extract, are bound to biomolecules attached to the surface (Pugazhendhi et al., 2018) ,(Arumai Selvan et al., 2018) (Figure 4C,D).

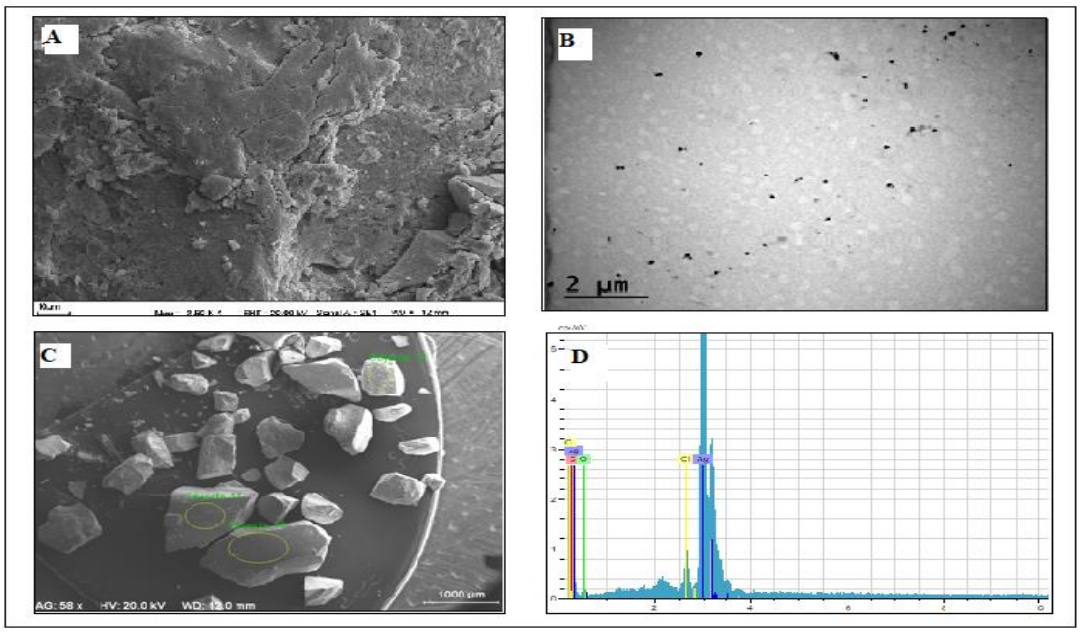

Figure 4. SEM-TEM and EDX micrographs of AgNPs **A.** SEM images, **B.** TEM images, **C, D.** EDX profile element composition graphs

3.5. Zeta potential distribution of AgNPs

According to Zeta potential analysis data, the distribution of surface charge of AgNPs was determined as -25.1 mV. The fact that AgNPs with a zeta potential distribution of -25.1 mV display only negative charge distribution shows that they do not have aggregation and exhibit a stable structure (Figure 5A). Negative and positive charge distribution of the surface charges of AgNPs causes aggregation of the particles (Al-ogaidi et al., 2017). The fact that the obtained AgNPs show only negative surface charge distribution indicates that there is no aggregation with the thrust effect of the same charge and they exhibit a stable structure (Patil et al., 2018), (Oliveira et al., 2019). In a study, the surface charges in the zeta potential distributions of AgNPs were stated as -29 mV (R. Nishanthi, S. Malathi, S. John Paul, 2019).

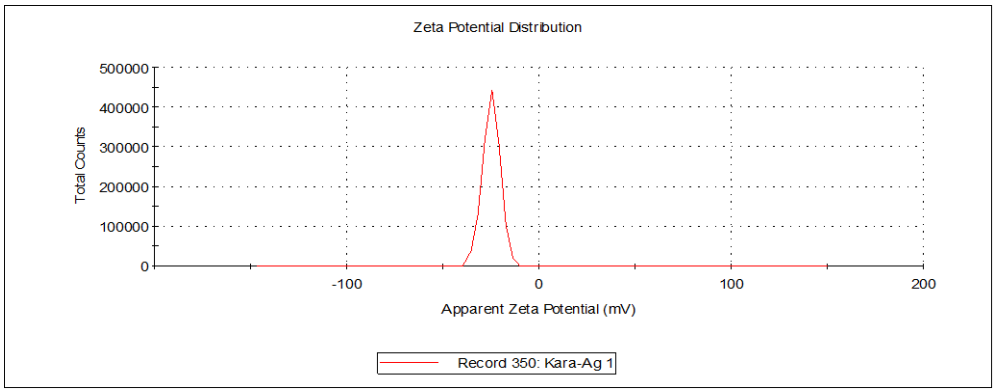

Figure 5. Zeta potential data showing the surface charge distributions of AgNPs

3.6. Anti-microbial Activities of AgNPs

Antimicrobial activities of AgNPs, antibiotics and 5 mM silver nitrate solution, which is the synthesis medium, on pathogenic microorganisms were evaluated by micro dilution method. It was determined that 0.03-0.12 µg/mL concentrations showed antimicrobial activity on the growth of microorganisms. The lowest concentration was determined as 0.03 µg/mL on *B. Subtilis* and *C. albicans* strains. The highest concentration is the MIC values effective on P. aeruginosa with a concentration of 0.12 µg/mL. Concentrations of 0.03-0.12 µg/mL are the MIC values obtained for all strains as lower concentrations of antibiotic and silver nitrate solution (Table 1 and Figure 7). The antimicrobial activities of AgNPs on microorganisms are caused by their high reactivity feature by being ionized in an aqueous environment. Ionized silver and microorganisms come into contact with the electrostatic attraction force (Kumar, R., Ghoshal, G. Jain, 2017), (Butola et al., 2019). After interaction, they increase Reactive Oxygen Species (ROS). With the increase of ROS, deterioration occurs in the structures of important biomolecules such as cell membrane and nucleus membrane (Rouhollah, H., and Marzieh, 2014). Biomolecules such as DNA, RNA and thiol groups of important enzymes have high affinity for ROS. They negatively affect the structure and functions of these molecules (Khan et al., 2018).

Tablo 1. MIC values of AgNPs, silver nitrate and antibiotics that show anti-microbial activity on microorganisms

ORGANISM	AgNPs µg/mL	Silver Nitrate µg/mL	Antibiotic µg/mL
S. aureus ATCC 29213	0.06	2.65	2.00
B.subtilis ATCC 11774	0.03	1.32	1.00
E. coli ATCC25922	0.06	0.66	2.00
P. aeruginosa ATCC27833	0.12	1.32	4.00
C. albicans	0.03	0.66	2.00

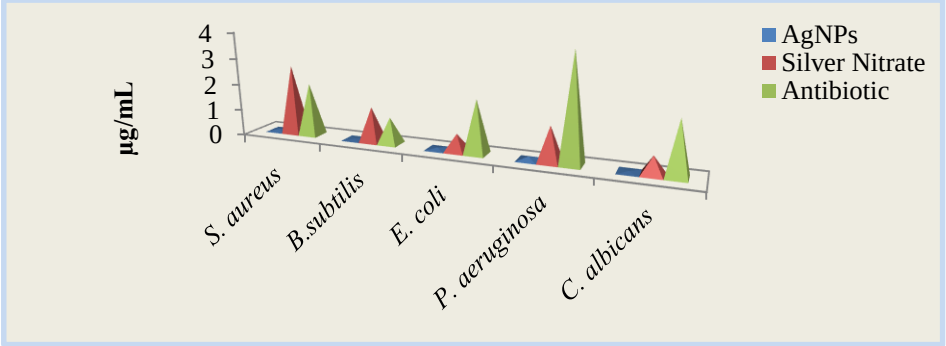

Figure 6. MIC values on which AgNPs, 5 mM AgNO3 solution and antibiotics are effective in antimicrobial activity on pathogenic microorganisms

In a study conducted for the anti-microbial effects of AgNPs obtained by biosynthesis on pathogenic strains *B. subtilis, S. aureus, E. coli, P. aeruginosa, C. albicans* at concentrations of 50, 50, 25, 50 and 25 µg / mL, respectively, were defined as MIC at antimicrobial activity (Emmanuel et al., 2015). In another study, 0.82 and 0.67 µg / mL concentrations were said to be effective for *S. aureus* and *E. coli* strains (V. Kumar et al., 2016).

3.7. Cytotoxic activities of AgNPs on cell lines

Cytotoxic activities and proliferation-inhibiting concentrations of AgNPs obtained by biosynthesis on healthy cell line HDF and cancer cell lines U118, CaCo-2 and Skov-3 were determined by MTT method. At 25 µg / mL, 42.53% viability and 57% suppressive toxic effects were detected on HDF cells. On U118, CaCo-2 and Skov-3 cell lines, 59.22%, 35.01 and 73.04% viability and 40, 64 and 26% suppressive toxic effect rates were determined, respectively, at a concentration of 25 µg/mL. In this case, it is seen that the highest suppressive effect of AgNPs with a rate of 64% is in the CaCo-2 cancer cell line (Table 2 and Figure 7). The increase in the percentage of viability versus the concentration of AgNPs in the cell lines is due to the proliferative properties of the cells (Morais et al., 2020).

AgNPs are laccolyzed in biomolecules at different points such as nucleus, mitochondria and cell membranes. Where they are localized, AgNPs stimulate apoptosis due to the increase in ROS. They show toxic effects

by inducing cell death (Gliga et al., 2014), (Morais et al., 2020). Ag^+ ions released as a result of AgNPs forming oxidative reactions can induce the formation of immunological and genotoxic structures in biological environments. It is important at this point to evaluate these effects with cytotoxic applications (Wongpreecha et al., 2018).

Table 2. Concentrations of AgNPs that suppress viability on cell lines

Cell Line	25 µg/mL	50 µg/mL	100 µg/mL	200 µg/mL
HDF	42.53	9.06	8.69	10.13
U118	59.22	61.08	62.82	56.46
CaCo-2	35.01	25.51	23.20	26.08
Skov-3	73.04	68.60	63.77	21.52

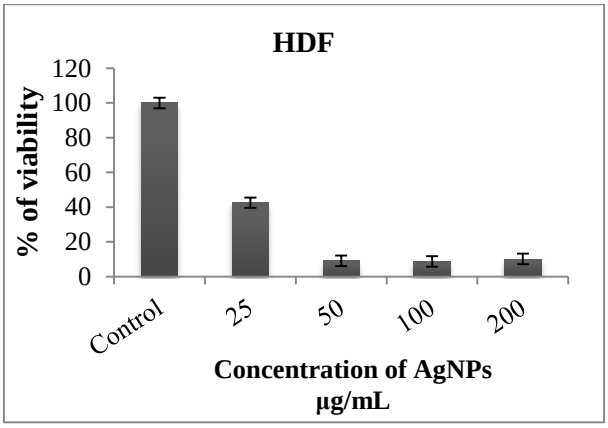

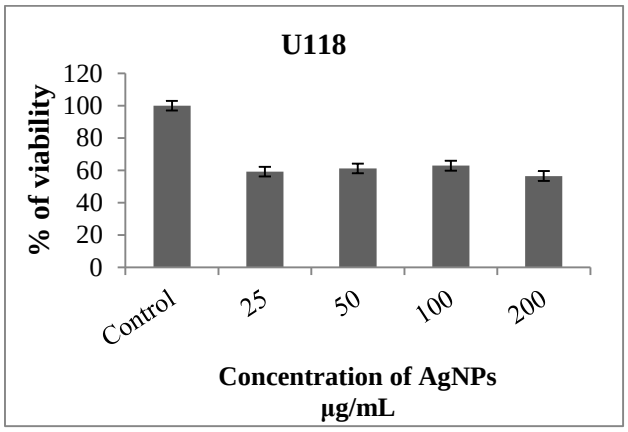

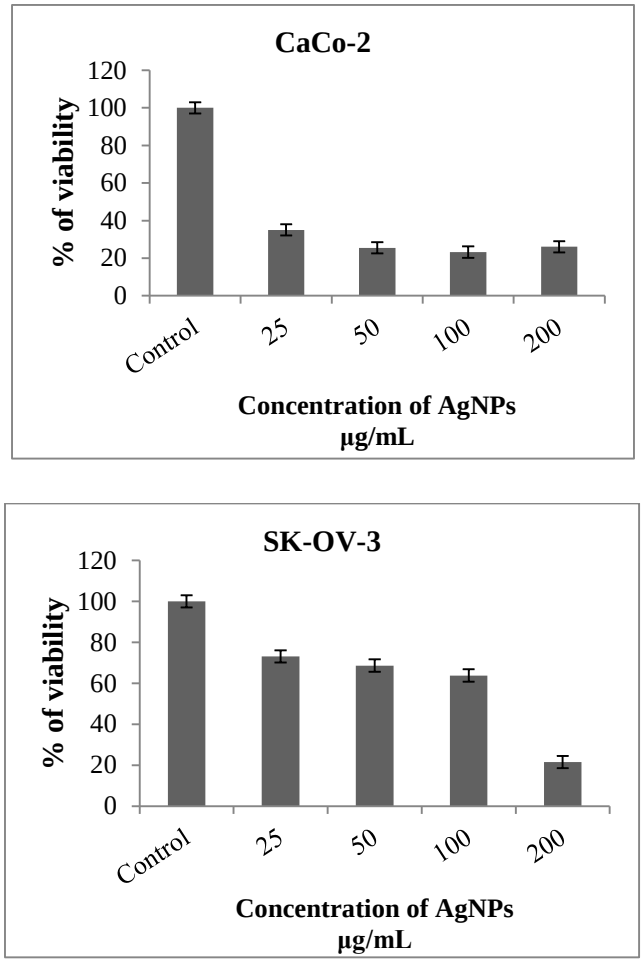

Figure 7. Percentage viability rates as a result of the growth-suppressing cytotoxic effects of AgNPs 48 hours after their interaction with HDF, CaCo-2, U118 and Skov-3 cell lines

In a study investigating the cytotoxic effects of AgNPs on CaCo-2 cells, it was stated that a concentration of 3.75 µg / mL has toxic effects (Mohmed et al., 2017). In another study, a concentration of 9.4 µg / mL was reported to be toxic in Skov-3 cell lines (Fahrenholtz et al., 2017). On the other hand, the determination of the cytotoxic effects of AgNPs on the HDF cell line It has been shown in a study conducted for 100 µg / mL concentration to have toxic effects (Yixia Zhang, Dapeng Yang, Yifei Kong, Xiansong Wang, Omar Pandoli, 2010).

There are some parameters that affect the toxic effect mechanism of nanoparticles. Among these, factors such as the concentration of nanoparticles, the chemistry of the surface components, surface charge, interaction time, size, degree of deposition, and shape are the factors in the formation of the toxic effect (Swamy et al., 2015).

CONCLUSION

The fact that AgNPs obtained by the biosynthesis method exhibit a biocompatible structure for biomedical applications makes these methods

interesting day by day. The biosynthesis of AgNPs with black mulberry leaf extract was carried out easily and economically. The AgNPs obtained are UV-vis. Spectrophotometer was characterized by XRD, FTIR, EDX, TEM, SEM, TEM and Zeta potential analysis data. It was determined that they exhibited antimicrobial activity at lower concentrations (0.03-0.12 µg / mL) against antibiotic and silver nitrate solution on pathogenic microorganisms. Cytotoxic effects and suppressive effects on cell growth were investigated by MTT method on healthy cell line HDF and cancer cell lines U118, CaCo-2 and Skov-3. It was determined that at a concentration of 25 µg / mL, the CaCo-2 cancer cell line showed the highest suppressive effect at a rate of 64%. In the synthesis, parameters such as concentration, pH, temperature, which determine the properties of AgNPs, can contribute greatly to the search for anticancer and antimicrobial agents for biomedical applications.

REFERENCES

Ahmed, M. J., Murtaza, G., Rashid, F., & Iqbal, J. 2019. Eco-friendly green synthesis of silver nanoparticles and their potential applications as antioxidant and anticancer agents. Drug Development and Industrial Pharmacy I, 45: 1682–1694.

Al-ogaidi, I., Salman, M. I., Mohammad, F. I., Aguilar, Z., Al-, M., Hadi, Y. A., & Al-rhman, R. M. A. 2017. Antibacterial and Cytotoxicity of Silver Nanoparticles Synthesized in Green and Black Tea. World Journal of Experimental Biosciences, 5(1): 39–45.

Ali, M. H. 2020. Eco-friendly synthesis of silver nanoparticles from crust of Cucurbita Maxima L. (red pumpkin). EurAsian Journal of BioSciences Eurasia J Biosci, 14(March), 2829–2833.

Ali, M., Kim, B., Belfield, K. D., Norman, D., Brennan, M., & Ali, G. S. 2016. Green synthesis and characterization of silver nanoparticles using Artemisia absinthium aqueous extract - A comprehensive study. Materials Science and Engineering C, 58, 359–365.

Ali, Z. A., Yahya, R., Sekaran, S. D., & Puteh, R. 2016. Green synthesis of silver nanoparticles using apple extract and its antibacterial properties. Advances in Materials Science and Engineering, 1–6.

Arroyo, G. V., Madrid, A. T., Gavilanes, A. F., Naranjo, B., Debut, A., Arias, M. T., & Angulo, Y. 2020. Green synthesis of silver nanoparticles for application in cosmetics. Journal of Environmental Science and Health - Part A Toxic/Hazardous Substances and Environmental Engineering, 55(11), 1304–1320.

Arumai Selvan, D., Mahendiran, D., Senthil Kumar, R., & Kalilur Rahiman, A. 2018. Garlic, green tea and turmeric extracts-mediated green synthesis of silver nanoparticles: Phytochemical, antioxidant and in vitro cytotoxicity studies. Journal of Photochemistry and Photobiology B: Biology, 180, 243–252.

Baran, M. F., Saydut, A. 2019. Gold nanomaterial synthesis and characterization. Dicle University Journal of Engineering, 10(3), 1033–1040.

Baran, M.F., Koç, A., and Uzan, S. 2018. Synthesis, Characterization and Antimicrobial Applications of Silver Nanoparticle (Agnp) with Kenger (Gundelia tournefortii) Leaf. International Journal on Mathematic, Engineering and Natural Sciences, 5: 44–52.

Baran, M. 2019. Synthesis of silver nanoparticles (AgNP) with Prunus avium cherry leaf extract and investigation of its antimicrobial effect. Dicle University Journal of Engineering, 10(1): 221–227.

Baran, M. F. 2018. Green Synthesıs of Sılver Nanopartıcles (AGNPs) Usıng Pıstacıa Terebınthus Leaf Extract: Antımıcrobıal Effect And Characterızatıon. International Journal on Mathematic, Engineering and Natural Sciences, 5(2): 67–75.

Butola, B. S., Gupta, A., & Roy, A. 2019. Multifunctional fi nishing of cellulosic fabric via facile , rapid in-situ green synthesis of AgNPs using pomegranate peel extract biomolecules. Sustainable Chemistry and Pharmacy, 12, 100135.

Doğaroğlu, Z. G., Eren, A., & Baran, M. F. 2019. Effects of ZnO Nanoparticles and Ethylenediamine- N, N ′- Disuccinic Acid on Seed Germination of Four Different Plants. Global Challanges, 1800111, 1–5.

El-Batal, A. I., Al-Hazmi, N. E., Mosallam, F. M., & El-Sayyad, G. S. 2018. Biogenic synthesis of copper nanoparticles by natural polysaccharides and Pleurotus ostreatus fermented fenugreek using gamma rays with antioxidant and antimicrobial potential towards some wound pathogens. Microbial Pathogenesis, 118(March), 159–169.

Emmanuel, R., Palanisamy, S., Chen, S., Chelladurai, K., Padmavathy, S., Saravanan, M., Prakash, P., Ali, M. A., & Al-hemaid, Fahad, M. A. 2015. Antimicrobial ef fi cacy of green synthesized drug blended silver nanoparticles against dental caries and periodontal disease causing microorganisms. Materials Science & Engineering C, 56, 374–379.

Eren, A., Baran, M. F. 2019a. Green Synthesıs , Characterızatıon And Antımıcrobıal Actıvıty Of Sılver Nanopartıcles (Agnps) From Maıze (*Zea mays* L .). Applıed Ecology and Envıronmental Research, 17(2), 4097–4105.

Eren, A., Baran, M. F. 2019b. Synthesis, Characterization and Investigation of Antimicrobial Activity of Silver Nanoparticles (AgNPs). Turkey Agricultural Research Journal, 6(2): 165–173.

Fahrenholtz, C. D., Swanner, J., Ramirez-Perez, M., & Singh, R. N. 2017. Heterogeneous Responses of Ovarian Cancer Cells to Silver Nanoparticles as a Single Agent and in Combination with Cisplatin. Journal of Nanomaterials, 1–11.

Ferreyra Maillard, A. P. V., Dalmasso, P. R., López de Mishima, B. A., & Hollmann, A. 2018. Interaction of green silver nanoparticles with model membranes: possible role in the antibacterial activity. Colloids and Surfaces B: Biointerfaces, 171(July), 320–326.

Francis, S., Joseph, S., Koshy, E. P., & Mathew, B. 2017. Green synthesis and characterization of gold and silver nanoparticles using Mussaenda glabrata leaf extract and their environmental applications to dye degradation. Environmental Science and Pollution Research, 24, 17347–17357.

Gliga, A. R., Skoglund, S., Wallinder, I. O., Fadeel, B., & Karlsson, H. L. 2014. Size-dependent cytotoxicity of silver nanoparticles in human lung cells: the role of cellular uptake, agglomeration and Ag release. Particle and Fibre

Toxicology, 11(1), 1–17.

Gopalu, K., Matheswaran J., Alexander, G., Juan, Antonio LT., Evgeny, K., D. K. 2016. Rapid Biosynthesis of AgNPs Using Soil Bacterium Azotobacter vinelandii With Promising Antioxidant and Antibacterial Activities for Biomedical Applications. The Journal of The Minerals, Metals & Materials Society, 69, 1206–1212.

Gupta, S. D., Agarwal, A., & Pradhan, S. 2018. Phytostimulatory effect of silver nanoparticles (AgNPs) on rice seedling growth: An insight from antioxidative enzyme activities and gene expression patterns. Ecotoxicology and Environmental Safety, 161: 624–633. h

Hafez, R. A., Abdel-wahhab, M. A., Sehab, A. F., & El-din, A. A. K. 2017. Green synthesis of silver nanoparticles using Morus nigra leave extract and evaluation their antifungal potency on phytopathogenic fungi. Journal of Applied Pharmaceutical Science, 7(02), 41–48.

Khan, A. U., Yuan, Q., Khan, Z. U. H., Ahmad, A., Khan, F. U., Tahir, K., Shakeel, M., & Ullah, S. 2018. An eco-benign synthesis of AgNPs using aqueous extract of Longan fruit peel: Antiproliferative response against human breast cancer cell line MCF-7, antioxidant and photocatalytic deprivation of methylene blue. Journal of Photochemistry and Photobiology B: Biology, 183: 367–373.

Kumar, R., Ghoshal, G. Jain, A. and G. M. 2017. Rapid Green Synthesis of Silver Nanoparticles (AgNPs) Using (Prunus persica) Plants extract: Exploring its Antimicrobial and Catalytic Activities. Journal of Nanomedicine & Nanotechnology, 8(4), 1–8.

Kumar, A., Kaur, K., & Sharma, S. 2013. Synthesis, characterization and antibacterial potential of silver nanoparticles by Morus nigra leaf extract. Indian Journal of Pharmaceutical and Biological Research, 1(04): 16–24.

Kumar, V., Gundampati, R. K., Singh, D. K., Bano, D., Jagannadham, M. V., Hasan, S.H. 2016. Photoinduced green synthesis of silver nanoparticles with highly effective antibacterial and hydrogen peroxide sensing properties. Journal of Photochemistry and Photobiology B: Biology, 162: 374–385.

Mohammadi, F., Yousefi, M., & Ghahremanzadeh, R. 2019. Green Synthesis , Characterization and Antimicrobial Activity of Silver Nanoparticles (AgNps) Using Leaves and Stems Extract of Some Plants. Advanced Journal of Chemistry-Section A, 2(4): 266–275.

Mohmed, A., Hassan, S., Fouda, A., Elgamal, M., & Salem, S. (2017). Extracellular Biosynthesis of Silver Nanoparticles Using Aspergillus sp. and Evaluation of their Antibacterial and Cytotoxicity. Journal of Applied Life Sciences International, 11(2): 1–12.

Morais, M., Teixeira, A. L., Dias, F., Machado, V., Medeiros, R., & Prior, J. A. V. 2020. Cytotoxic Effect of Silver Nanoparticles Synthesized by Green Methods in Cancer. Journal of Medicinal Chemistry, 63(23): 14308–14335.

Mousavi, S. A., Almasi, A., Navazeshkh, F., & Falahi, F. 2019. Biosorption of lead from aqueous solutions by algae biomass: Optimization and modeling. Desalination and Water Treatment, 148, 229–237.

Ojo, O.A., Oyinloye, B.E., Ojo, A.B., Afolabi, O.B., Peters, O.A., Olaiya, O., Fadaka, A., Jonathan, j., Osunlana, O. 2017. Green Synthesis of Silver Nanoparticles (AgNPs) Using Talinum triangulare (Jacq .) Willd . Leaf Extract and Monitoring Their Antimicrobial Activity. Journal of Bionanoscience, 11, 292–296.

Oliveira, A. C. de J., Araújo, A. R. de, Quelemes, P. V., Nadvorny, D., Soares-Sobrinho, J. L., Leite, J. R. S. de A., da Silva-Filho, E. C., & Silva, D. A. da. 2019. Solvent-free production of phthalated cashew gum for green synthesis of antimicrobial silver nanoparticles. Carbohydrate Polymers, 213, 176–183.

Patil, M. P., Singh, R. D., Koli, P. B., Patil, K. T., Jagdale, B. S., Tipare, A. R., & Kim, G. (2018). Antibacterial potential of silver nanoparticles synthesized using Madhuca longifolia flower extract as a green resource. Microbial Pathogenesis, 121: 184–189.

Pugazhendhi, S., Palanisamy, P. K., & Jayavel, R. 2018. Synthesis of highly stable silver nanoparticles through a novel green method using Mirabillis jalapa for antibacterial, nonlinear optical applications. Optical Materials, 79: 457–463.

R. Nishanthi, S. Malathi, S. John Paul, P. P. 2019. Green synthesis and characterization of bioinspired silver, gold and platinum nanoparticles and evaluation of their synergistic antibacterial activity after combining with different classes of antibiotics. Materials Science and Engineering: C, 96: 693–707.

Ramkumar, V. S., Pugazhendhi, A., Gopalakrishnan, K., Sivagurunathan, P., Saratale, G. D., Dung, T. N. B., & Kannapiran, E. (2017). Biofabrication and characterization of silver nanoparticles using aqueous extract of seaweed Enteromorpha compressa and its biomedical properties. Biotechnology Reports, 14, 1–7.

Remya, R. R., Rajasree, S. R. R., Aranganathan, L., & Suman, T. Y. 2015. An investigation on cytotoxic effect of bioactive AgNPs synthesized using Cassia fistula flower extract on breast cancer cell MCF-7. Biotechnology Reports, 8, 110–115.

Rouhollah, H., and Marzieh, R. 2014. Biosynthesis of silver nanoparticles using extract of olive leaf : synthesis and in vitro cytotoxic effect on MCF-7 cells. International Journal OfBreast Cancer, 1–7.

S, Majeed., Mohd, S. A., Gouri K. D., Mohammed, T.A., Anima, N. (2016). Biochemical synthesis of silver nanoprticles using filamentous fungi Penicillium decumbens (MTCC-2494) and its efficacy against A-549 lung cancer cell line. Chinese Journal of Natural Medicines, 14(8): 615–620.

Shao, Y., Wu, C., Wu, T., Yuan, C., Chen, S., Ding, T., Ye, X., & Hu, Y. 2018. Green synthesis of sodium alginate-silver nanoparticles and their antibacterial activity. International Journal of Biological Macromolecules, 111: 1281–1292.

Singh, J., Mehta, A., Rawat, M., & Basu, S. 2018. Green synthesis of silver nanoparticles using sun dried tulsi leaves and its catalytic application for 4-Nitrophenol reduction. Journal of Environmental Chemical Engineering, 6: 1468–1474.

Song, J. Y., & Kim, B. S. 2009. Rapid biological synthesis of silver nanoparticles using plant leaf extracts. Bioprocess and Biosystems Engineering, 32(1): 79–84.

Swamy, M. K., Akhtar, M. S., Mohanty, S. K., & Sinniah, U. R. 2015. Synthesis and characterization of silver nanoparticles using fruit extract of Momordica cymbalaria and assessment of their in vitro antimicrobial, antioxidant and cytotoxicity activities. *Spectrochimica Acta - Part A:* Molecular and Biomolecular Spectroscopy, 151: 939–944.

Thomas, B., Vithiya, B. S. M., Prasad, T. A. A., Mohamed, S. B., Magdalane, C. M., Kaviyarasu, K., & Maaza, M. (2018). Antioxidant and Photocatalytic Activity of Aqueous Leaf Extract Mediated Green Synthesis of Silver Nanoparticles Using Passiflora edulis f. flavicarpa. Journal of Nanoscience and Nanotechnology, 19(5): 2640–2648.

Vastrad, J. 2016. Green Synthesis and Characterization of Silver Nanoparticles Using Leaf Extract of Tridax Procumbens. Asian Journal of Pharmaceutical and Research, 7(2): 44–48.

Velmurugan, P., Anbalagan, K., Manosathyadevan, M., Lee, K. J., Cho, MinJung-Hee Park, Sae-Gang Oh, K.-S. B., Oh, B.-T., & Lee, S. M. 2014. Green synthesis of silver and gold nanoparticles using Zingiber officinale root extract and antibacterial activity of silver nanoparticles against food pathogens. Bioprocess and Biosystems Engineering, 37(10): 1935–1943.

Wongpreecha, J., Polpanich, D., Suteewong, T., Kaewsaneha, C., & Tangboriboonrat, P. (2018). One-pot, large-scale green synthesis of silver nanoparticles-chitosan with enhanced antibacterial activity and low cytotoxicity. Carbohydrate Polymers, 199(July), 641–648.

Yixia Zhang, Dapeng Yang, Yifei Kong, Xiansong Wang, Omar Pandoli, G. G. (2010). Synergetic Antibacterial Effects of Silver Nanoparticles@Aloe Vera Prepared via a Green Method. Nano Biomedical Engineering, 2(4): 252–257.